Orientational Disorder and Entropy of Water in Protein Cavities

Vladimir P. Denisov,[†] Kandadai Venu,[†,‡] Jörg Peters,[§] Hans Dietrich Hörlein,[§] and Bertil Halle*[,†]

Condensed Matter Magnetic Resonance Group, Department of Chemistry, Lund University, P.O. Box 124, S-22100 Lund, Sweden, and Bayer AG, PH-TO Biotechnologie, D-42096 Wuppertal, Germany

Received: April 9, 1997[⊗]

Water ^{17}O, ^{2}H, and ^{1}H nuclear magnetic relaxation dispersion (NMRD) data are presented for the Y35G mutant of bovine pancreatic trypsin inhibitor (BPTI) in aqueous solution. The NMRD data show that the three buried water molecules in this protein exchange with bulk water on the time scale of 15 ns to 1 μs and undergo librational motion of considerable amplitude in the protein cavities. By analysis of the three independent order parameters provided by the NMRD data in terms of an anisotropic harmonic libration model, the amplitude and anisotropy of water rotation in protein cavities is quantitatively assessed. All seven distinct buried water molecules in wild-type BPTI and in the G36S and Y35G mutants are examined in this way. The harmonic libration model also allows the rotational entropy of buried water molecules to be deduced from the experimental order parameters. Although each of the investigated buried water molecules is engaged in three or four hydrogen bonds, their entropies span the full range from ice to bulk water, suggesting that the hydration of protein cavities with weaker hydrogen-bonding capacity may be entropically driven. This might be true also for weakly hydrogen-bonded water molecules in surface clefts, thus reversing the conventional view that ligand binding to proteins is entropically favored by release of ordered water.

Introduction

Internal cavities large enough to accomodate at least one water molecule are found in nearly all globular proteins, typically accounting for 1 % of the protein volume.[1−4] In crystal structures, some of these cavities are occupied by translationally ordered water molecules, while other cavities appear to be empty.[5−7] Protein cavities may be viewed as structural defects, resulting from the conflicting requirements of hydrogen-bonded secondary structure elements and a uniformly high packing density. It is becoming increasingly clear, however, that cavities can be directly involved in protein function. Empty cavities can facilitate transport of small substrates through the protein matrix[8,9] or can enable large-scale domain movements.[10,11] Hydrated protein cavities, i.e., internal (or buried) water molecules, can be directly involved in enzyme catalysis[12] and ligand binding.[13,14] An improved understanding of internal hydration should also have important implications for the broader issues of folding and stability of globular proteins.

The current knowledge about buried water molecules in proteins is largely derived from high-resolution X-ray diffraction data.[5,6] In recent years, information about buried water molecules has also come from high-resolution ^{1}H NMR studies of intermolecular nuclear Overhauser effects (NOEs)[15−17] and from water ^{17}O and ^{2}H nuclear magnetic relaxation dispersion (NMRD) studies.[18−20] Although not competitive with crystallography in terms of structural detail, the NMR methods have distinct advantages in other respects. First, they report on proteins in aqueous solution, which is usually the physiological medium. Second, the NOE method can detect cavity water at occupancies as low as 10%,[21] whereas the detection limit of X-ray diffraction is typically 30−50%. (Owing to a strong correlation between the occupancy and the thermal *B* factor, occupancies of all detected buried water moelcules are usually fixed at 100% during refinement.[5,6]) Third, the NMRD method provides intramolecular order parameters reflecting the orientational fluctuations of buried water molecules, information that is not readily extracted even from neutron diffraction data.[7] Fourth, both NMR methods provide information about the rate of exchange of water molecules between protein cavities and bulk water, whereas conventional crystallography can provide only equilibrium averages. The dynamic information is most directly manifested in NMRD data, which probe the fluctuation spectrum over a wide frequency range. The rate at which a water molecule escapes from a protein cavity is of interest mainly because it reflects large-scale structural fluctuations that are thought to be rate-limiting for exchange of deeply buried water molecules.[22]

Another important aspect of cavity hydration concerns the relation between structure and thermodynamics. When this relationship is understood, it should be possible, given the structure of a protein cavity, to predict its occupancy and the consequent stabilization of the native protein structure. Considering the marginal stability with respect to unfolding of most globular proteins under physiological conditions, cavity hydration may well be an important stabilizing factor. The available crystallographic data show that most buried water molecules engage in three or four hydrogen bonds to protein O and N atoms lining the cavity,[3,5] suggesting rather stringent requirements for cavity hydration. This picture is supported by free energy calculations based on atomic force fields[23,24] and by considerations of the solubility of water in nonpolar solvents.[25] Yet, water molecules have also been detected, by X-ray crystallography[3,6,26] and by the NOE method,[21,27] in essentially nonpolar cavities, suggesting rather less stringent hydrogen-bond requirements. Since positional disorder (large *B* factor) and/or partial occupancy may render such buried water molecules X-ray-invisible, their prevalence may have been underestimated.

Experimental data on the thermodynamics of cavity hydration in proteins are scarce. The order parameters obtained from

[†] Lund University.

[‡] Permanent address: School of Physics, University of Hyderabad, Hyderabad 500046, India.

[§] Bayer AG.

[⊗] Abstract published in *Advance ACS Abstracts,* October 1, 1997.

S1089-5647(97)01221-2 CCC: $14.00

NMRD studies, however, reflect the local orientational distribution function that governs the configurational part of the rotational entropy.[28,29] This link between NMR-derived order parameters and rotational entropy has previously been explored for orientational fluctuations of N−H and C−H bonds in the polypeptide backbone[30,31] and in side chains.[32] The case of water is different in several respects. First, the entropy of a buried water molecule directly affects an observable property, the cavity occupancy. Second, since the nuclear spin coupling tensors of ^{17}O, ^{2}H, and ^{1}H are differently oriented in the water molecule, multinuclear NMRD data can provide three independent order parameters, characterizing the anisotropy of the local water reorientation.[33,34] Third, the translational degrees of freedom of a buried water molecule also contribute to the entropy. Our analysis indicates, however, that this contribution is less important than the rotational one, at least for the buried water molecules considered here.

Among the several globular proteins so far studied by multinuclear water NMRD,[20] the best characterized is bovine pancreatic trypsin inhibitor (BPTI). NMRD data for all three water nuclei have been reported for wild-type BPTI,[18,34,35] with four buried water molecules,[36] and for the mutant G36S,[19,22,34] where one of the four is replaced by the hydroxyl group of Ser-36.[37] Here, we report a complete set of water NMRD curves for another BPTI mutant, Y35G, which has three buried water molecules in cavities distinct from those in wild-type BPTI.[38] The combined NMRD data for wild-type BPTI and the two mutants, comprising seven distinct buried water molecules, are then analyzed in terms of an anisotropic harmonic libration (AHL) model, allowing us to convert the ^{17}O, ^{2}H, and ^{1}H order parameters to fluctuation amplitudes for the rock, wag, and twist libration modes. The theoretical basis for this analysis is presented in the Appendix. Although the singly buried water molecule (W122) in wild-type BPTI has an orientational order comparable to that in ice, the other buried water molecules are found to be more disordered, with rms libration amplitudes as large as 30°. Moreover, the three buried water molecules in Y35G are found to be more disordered than the three in G36S.

In the final stage of the analysis, we use the AHL model to convert the libration amplitudes to rotational entropy contributions. The results indicate that the entropy of the buried water molecules in Y35G is comparable to that of bulk water, suggesting that the hydration of cavities with weaker hydrogen-bonding capacity may be entropically driven. Enthalpy−entropy compensation thus appears to be an important feature of cavity hydration, as in many other processes that involve restructuring of hydrogen bonds in aqueous media at ambient temperature.[39,40] It is widely believed that the release of ordered water contributes significantly to the driving force for protein−ligand and protein−receptor association in aqueous solution. This is also the conventional view of the hydrophobic effect. The scenario that we propose for weakly hydrogen-bonded cavity water is the opposite one, where dehydration reduces the entropy of water. Similarly, ligand binding to pockets and crevices at the protein surface may be entropically disfavored by the displacement of weakly hydrogen-bonded water molecules.

Materials and Methods

Materials. The BPTI mutant Met(-1)-Y35G was prepared according to the procedure described earlier for the G36S mutant.[37] A cell-free yeast culture was adjusted to pH 3 with citric acid and diluted with water to a final conductivity of 11 mS cm^{-1}, whereafter 200 mL SP-Sepharose FF (Pharmacia, Uppsala) was added and incubated for 50 min. The resin was washed first with 3 L of 50 mM citrate−NaOH buffer (pH 3), then with 2 L of 50 mM Tris-HCl (pH 9), and finally with 2 L of 20 mM HEPES (pH 6). After the gel was packed into a column, the Y35G mutant was eluted by a linear salt gradient (0−1 M NaCl, 20 mM HEPES, pH 6). Fractions (20 mL) were taken and pooled according to reversed-phase HPLC analysis. Fractions containing the product were pooled, adjusted to pH 3 (citric acid), diluted to a final conductivity of 23 mS cm^{-1}, and passed through a 0.22 μm filter (Sartorius, Göttingen). This solution was pumped onto a 100 mL S-Sepharose HP column (Pharmacia, Uppsala) previously equilibrated with 3 column volumes of citrate−NaOH buffer (50 mM, pH 3). The adsorbed product was washed with 470 mL of starting buffer and then with 20 mM HEPES (pH 6). Elution of the Y35G mutant was performed using a linear salt gradient (20 mM HEPES/0−1 M NaCl, pH 6). Fractions (20 mL) were taken for RP-HPLC analysis, and those containing the product were pooled and filtered (0.22 μm). As the final purification step, the S-Sepharose-HP pool was chromatographed on a preparative Vydac C18-HPLC column (40 mL) previously equilibrated with 0.1% trifluoroacetic acid. The product was eluted using a linear gradient of acetonitrile. Fractions containing the Y35G mutant were pooled, diluted with water, and lyophilized. The final product was characterized by N-terminal sequencing over 39 cycles, capillary electrophoresis (yielding a homogeneous peak), amino acid analysis (in agreement with calculated values), and native PAGE (yielding a homogeneous peak). The purified protein preparation, lyophilized as a salt of trifluoroacetic acid, contained 99.7% Y35G according to results of SDS-PAGE and RP-HPLC.

Protein solutions were made by dissolving the lyophilized protein in heavy water (molar mass 21.5 g mol^{-1}), enriched in ^{17}O (Ventron, 21.9 atom % ^{17}O, 61.9 atom % ^{18}O, 99.95 atom % ^{2}H), or doubly distilled water. The operational pH* (without isotope correction) was adjusted to 5.2 by adding small amounts of concentrated NaOH or KOH. Protein concentrations were determined on the basis of complete amino acid analysis, yielding 23.1 ± 0.5 mM for the D_2O sample.

Relaxation Dispersion Measurements. Oxygen-17, deuteron, and proton relaxation rates were measured at different magnetic field strengths as described previously,[19,34] using four Bruker and Varian NMR spectrometers and an iron magnet (Drusch EAR-35N) equipped with field-variable lock and flux stabilizer. The sample temperature was maintained at 27.0 ± 0.1 °C by a thermostated air flow.

Results and Discussion

Water Relaxation Dispersions. The longitudinal magnetic relaxation rates of the water ^{17}O, ^{2}H, and ^{1}H nuclei in aqueous protein solutions typically exhibit a dispersion in the megahertz range, with a dispersion frequency that reflects the rotational diffusion (correlation time τ_R) of the protein. The ^{17}O dispersion is produced by a small number of water molecules with residence times longer than τ_R but shorter than the intrinsic spin relaxation time.[18−20] When ^{17}O NMRD data from a variety of proteins are correlated with high-resolution crystal structures, it is found that such long-lived water molecules are either trapped in cavities or deep crevices or coordinated to protein-bound multivalent metal ions.[20] The ^{2}H and ^{1}H dispersions generally contain a contribution from labile protein hydrogens, in addition to that from long-lived water molecules.[34,35] In the case of BPTI, the labile hydrogen contribution to the ^{2}H dispersion is negligible at pH 5−6 [35] but is substantial at all pH values for the more slowly relaxing ^{1}H nucleus.[34]

Wild-type BPTI contains four buried water molecules.[36] One of these (denoted W122) resides in an isolated cavity near the

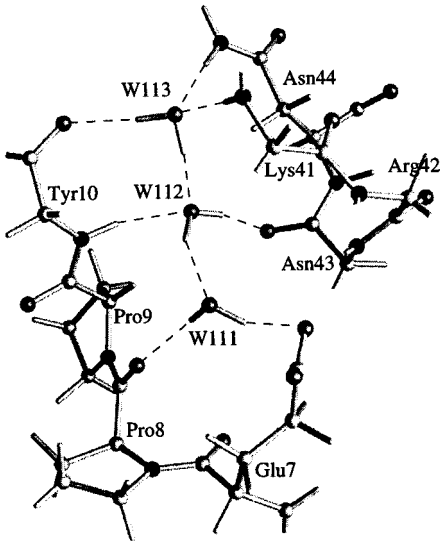

Figure 1. Hydrogen-bond geometry for the buried water molecules W111−W113 in the crystal structure 5pti of wild-type BPTI,[36] which is nearly identical to the solution structures of BPTI and G36S.[37,41]

14−38 disulfide bridge, while the other three (W111−W113) occupy a porelike cavity between the two major loops of the polypeptide chain (see Figure 1). In the mutant G36S, W122 is replaced by the hydroxyl group of the Ser-36 side chain with little structural perturbation elsewhere in the protein.[37] Previous difference-NMRD studies of wild-type BPTI and the G36S mutant have established that W122 exchanges relatively slowly with a residence time of 170 ± 20 μs at 300 K.[22] Since this is comparable to the intrinsic relaxation time for ^{2}H but much shorter/longer than that for ^{1}H/^{17}O, W122 contributes fully only to the ^{1}H dispersion at this temperature.[22,34] After subtraction of the labile-proton contribution to the ^{1}H relaxation, the ^{17}O, ^{2}H, and ^{1}H dispersions from G36S were found to be consistent with a contribution from three water molecules, with residence times in the range of 15 ns of 1 μs and with fast librational motions of modest amplitude.[19,22,34] Although not demonstrated directly by a difference-NMRD experiment (as for W122), the crystal structure strongly suggests that this contribution is due to the buried water molecules W111−W113. The only other plausible candidate is W143, residing in a surface pocket with three hydrogen bonds to the protein. Compared to W111 (at the mouth of the pore), however, W143 is more exposed to bulk solvent (the pocket is not as deep) and has longer (weaker) hydrogen bonds. Both these factors should reduce the residence time of W143 compared to the case of W111.[20] Indeed, high-resolution ^{1}H NMR studies of intermolecular NOEs between BPTI and water indicate that W143 has a subnanosecond residence time even at 4 °C.[16] In conclusion, only three water molecules, viz. W111−W113, contribute to the ^{17}O, ^{2}H, and ^{1}H dispersions from the G36S mutant.

The BPTI mutant Y35G, with the bulky side chain of Tyr-35 replaced by a hydrogen atom, shows an unusually large structural perturbation for a single-site mutation.[38] Although the main fold of the polypeptide chain and about two-thirds of the protein structure (including the hydrophobic core) are highly conserved, the two major loops are substantially rearranged compared to that of wild-type BPTI (rms deviations of 2 and 4 Å).[38] As a result, none of the four buried water molecules in wild-type BPTI is strictly conserved in Y35G. A new cavity occupied by two buried water molecules (W301 and W302) is created near the mutation site, while a third buried water molecule (W303) corresponds roughly (rms deviation 1.3 Å) to W111 in wild-type BPTI (cf. Figures 1 and 2b).[38] The

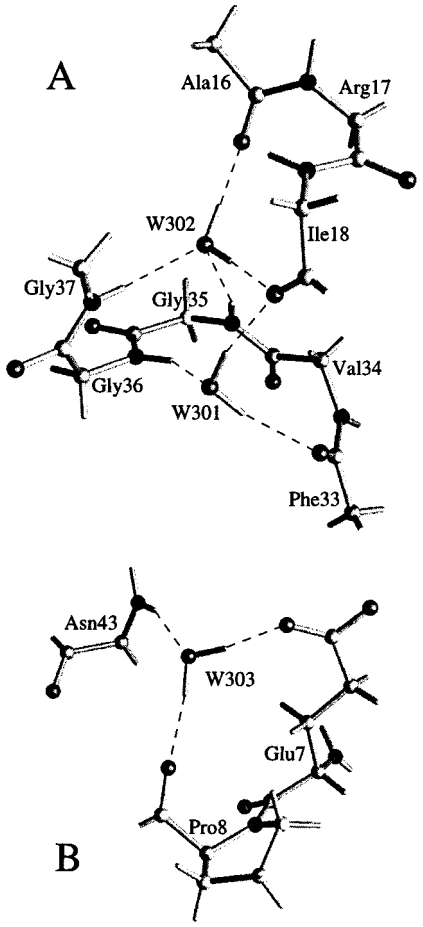

Figure 2. Hydrogen-bond geometry for the buried water molecules W301−W302 (A) and W303 (B) in the crystal structure 8pti of the BPTI mutant Y35G.[38] Hydrogen atoms have been added assuming standard intramolecular geometry and optimal hydrogen bonds.

TABLE 1: Hydrogen Bond Lengths for Buried Water Molecules in Wild-Type BPTI and in the Y35G Mutant

BPTI water[a]	partner	R_{OX} (Å)	Y35G water[b]	partner	R_{OX} (Å)
W113	W112	2.6	W301	Ile-18 CO	2.9
	Tyr-10 CO	2.9		Phe-33 CO	3.0
	Asn-44 NH_2	2.9		Gly-36 NH	2.7
	Lys-41 NH	3.0			
W112	W111	2.9	W302	Ile-18 CO	2.8
	Asn-43 CO	2.8		Ala-16 CO	2.7
	W113	2.6		Gly-35 NH	3.0
	Tyr-10 NH	2.9		Gly-37 NH	3.0
W111	Glu-7 CO_2	2.6	W303	Glu-7 CO_2	2.7
	Pro-8 CO	2.7		Pro-8 CO	3.0
	W112	2.9		Asn-43 NH	3.1

[a] Based on PDB file 5pti (wild-type BPTI in crystal form II).[36] [b] Based on PDB file 8pti (Y35G mutant).[38]

solution structure of Y35G has not been determined but is probably close to the crystal structure as for wild-type BPTI and G36S.[37,41] On the other hand, chemical shift, hydrogen exchange, and ^{15}N relaxation studies on Y35G in solution indicate that Y35G has a more flexible structure than wild-type BPTI.[42,72] The unfolding temperature is lowered by nearly 20 °C, corresponding to ca. 5 kcal mol^{-1} destablization of the native structure.[42] The hydrogen-bond geometries for W111−W113 in wild-type BPTI (assumed to be the same in G36S) and for W301−W303 in Y35G are shown in Figures 1 and 2, while the relevant hydrogen-bond lengths are compiled in Table 1.

Figure 3 shows the water ^{17}O, ^{2}H, and ^{1}H relaxation dispersion curves from solutions of Y35G at pH* 5.2. For

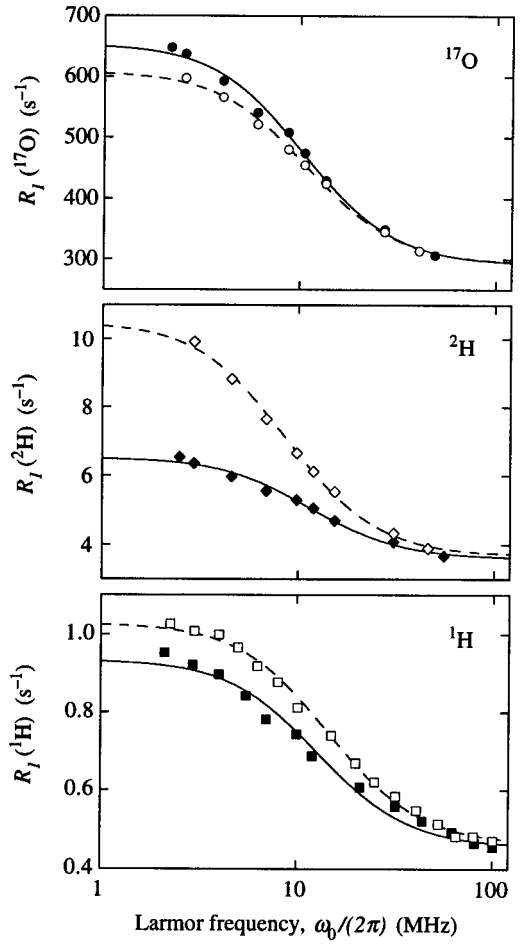

Figure 3. Dispersion of the water ^{17}O (top), ^{2}H (middle), and ^{1}H (bottom) longitudinal relaxation rates in D_2O (^{17}O, ^{2}H) or H_2O (^{1}H) solutions (27 °C, pH* 5.2) of the BPTI mutant Y35G (filled symbols and solid curves). The corresponding data[19,34] for the G36S mutant, scaled to the Y35G concentration, are also shown (open symbols and dashed curves). The estimated error bars are roughly twice the size of the data symbols. The curves resulted from fits of the parameters R_{hf}, β, and τ_c in eq 1 to the experimental data.

comparison, we have included the corresponding dispersion curves for G36S[19,34] (scaled to the Y35G concentration). The data are well represented by the theoretical expression[43−45]

$$R_1(\omega_0) = R_{hf} + \beta\tau_c\left[\frac{0.2}{1+(\omega_0\tau_c)^2} + \frac{0.8}{1+(2\omega_0\tau_c)^2}\right] \quad (1)$$

where ω_0 is the Larmor frequency and τ_c is the effective correlation time for the buried water molecules, which here can be identified with the rotational correlation time τ_R of the protein (vide infra). The dispersion amplitude β is due to buried water molecules (and, for ^{1}H, to labile protons), while the high-frequency relaxation rate $R_{hf} \equiv R_1(\omega_0 \gg 1/\tau_c)$ represents the contribution from all external water molecules in the bulk and at the protein surface. The parameters R_{hf}, β, and τ_c, determined from the nonlinear least-squares fits shown in Figure 3, are collected in Table 2, together with the corresponding values for G36S.[19,34]

The similarity of the two mutants with respect to the high-frequency plateau (R_{hf}) and the dispersion frequency (τ_c) is consistent with a similar surface (on average) and shape for the two proteins, as expected from the crystal structures. The correlation times τ_c obtained from the ^{17}O and ^{1}H dispersions differ by a factor of 1.23 ± 0.08, close to the ratio of the solvent viscosities (1.27) in the D_2O and H_2O samples. This is consistent with the identification of τ_c as the rotational correlation time τ_R of the protein.

TABLE 2: Water ^{17}O, ^{2}H, and ^{1}H NMRD Parameters for the Y35G and G36S Mutants of BPTI in Aqueous Solution at pH* 5.2 and 27 °C[a]

mutant	R_{hf} (s^{-1})	β (10^8 s^{-2})	τ_c (ns)
		^{17}O	
G36S	294 ± 4	387 ± 15	8.3 ± 0.3
Y35G	291 ± 3	417 ± 15	8.7 ± 0.3
		^{2}H	
G36S	3.68 ± 0.04	6.50 ± 0.15	10.5 ± 0.3
Y35G	3.60 ± 0.04	3.70 ± 0.15	7.9 ± 0.3
		^{1}H	
G36S	0.464 ± 0.002	0.91 ± 0.03	6.2 ± 0.2
Y35G	0.456 ± 0.002	0.68 ± 0.02	7.1 ± 0.2

[a] The original[19,34] R_{hf} and β values for G36S have been scaled to the Y35G concentration using scaling factors 1.019 (^{17}O, ^{2}H) and 1.444 (^{1}H).

For the analysis of the amplitudes of the ^{17}O, ^{2}H, and ^{1}H dispersions, it is convenient to scale the relaxation rates according to[19,34]

$$R_1^{scaled} \equiv [R_1(\omega_0) - R_{hf}]N_T/(C\tau_c) \quad (2)$$

where N_T is the water-to-protein mole ratio (i.e., a concentration factor) and C is a nuclear spin coupling factor equal to $(12\pi^2/125)\chi^2$ for ^{17}O, $(3\pi^2/2)\chi^2$ for ^{2}H, and $(^{10}/_{3})M_2$ for ^{1}H, with χ the quadrupole coupling constant and M_2 the (total) dipolar second moment.[43] Since the buried water molecules are extensively hydrogen bonded, these coupling constants should not deviate much from their values in ice Ih:[18,19,34] $\chi(^{17}O) = 6.5$ MHz,[46] $\chi(^{2}H) = 213$ kHz,[47] and $M_2 = 32.4$ G^2.[48] With these parameter values and with R_{hf} and τ_c values from Table 2, we obtain the scaled dispersion curves in Figure 4.

For the ^{2}H and ^{17}O dispersions, which are free from labile-hydrogen contributions, the amplitude parameter β can be expressed as[18,20]

$$\beta = (N/N_T)\langle CA^2\rangle \quad (3)$$

with N_T the total number of water molecules per protein molecule in the sample as calculated from the protein concentration. For the Y35G samples, $N_T = 2140$. Furthermore, N is the number of water molecules contributing to the dispersion and A their (rms) generalized orientational order parameter.[18,20] According to eqs 1−3, the low-frequency plateau of the scaled ^{2}H and ^{17}O dispersion directly yields the quantity NA^2. Since $A < 1$ (vide infra), the observed NA^2 values close to 2 (cf. Figure 4) are consistent with three long-lived water molecules for both mutants. Strictly speaking, this is only a lower bound on N, but since there are only three buried water molecules in the crystal structures and no indications of further potentially long-lived water molecules (cf. the preceding discussion for G36S), we can safely set $N = 3$ for both mutants. It follows directly from the NMRD data that the residence times of these water molecules must fall within the ^{17}O NMRD window,[20] 15 ns to 1 μs. A shorter residence time would reduce τ_c, while a longer residence time would suppress the ^{17}O dispersion amplitude (vide infra).[20]

Comparing the dispersion amplitudes for the three nuclei, we note that, for G36S, the ^{1}H amplitude is considerably larger than the coincident ^{2}H and ^{17}O amplitudes. This difference is essentially due to a labile-proton contribution,[34] which should

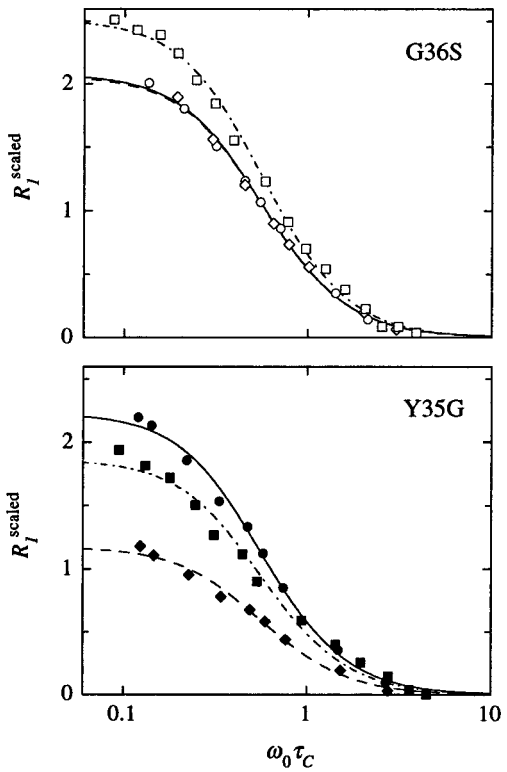

Figure 4. Same ^{17}O (●, ○, solid curves), ^2H (◆, ◇, dashed), and ^1H (■, □, dash−dot) data as in Figure 3 but scaled according to eq 2 and presented separately for the G36S (top) and Y35G (bottom) mutants.

also be present for Y35G. When this contribution is subtracted, a striking difference between the two mutants is evident. Whereas the three (hydrogen-exchange corrected) amplitudes are similar for G36S, they differ substantially for Y35G. This indicates that the librational motions of the buried water molecules are significantly different in the two mutants. The quantitative analysis that follows also shows that the average libration amplitude is larger in Y35G than in G36S, consistent with the more labile structure of Y35G in solution.[42]

Order Parameters of Buried Water Molecules. For the scaling in Figure 4, we used quadrupole coupling constants χ for ice Ih. For a quantitative interpretation of the order parameters A in terms of libration amplitudes, however, it is more appropriate to use a (hypothetical) rigid-lattice coupling constant. From an approximate decomposition of the librational IR band, the rms libration amplitude of the water molecules in ice Ih has been estimated to 8° (essentially isotropic and independent of temperature).[49] The quadrupole (or electric field gradient) tensor deduced from NQR or single-crystal NMR studies of ice[46,47] can thus be regarded as motionally averaged by three Gaussian libration modes of 8° rms amplitude. A straightforward calculation shows that the rigid-lattice quadrupole coupling constants should then exceed the quoted values by 6%. The asymmetry parameters, $\eta(^2H) = 0.11$ and $\eta(^{17}O) = 0.93$,[46,47] are unaffected by isotropic librational motions.

A further minor complication is that the quadrupole coupling constants depend somewhat on the hydrogen bond geometry.[50,51] For all the buried water molecules considered here, both water hydrogens are hydrogen-bonded to oxygen atoms (belonging to the protein or to another buried water molecule). Using an empirical correlation[50] between the deuteron quadrupole coupling constant $\chi(^2H)$ and the O−O separation R_{OO} (see Table 1), we obtain for the three buried water molecules (six deuterons) in Y35G $\chi(^2H) = 235$ kHz and for the three buried water molecules in G36S $\chi(^2H) = 218$ kHz. (These are rms values.)

TABLE 3: Generalized Order Parameters for Buried Water Molecules in Wild-Type BPTI and in the G36S and Y35G Mutants[a]

nucleus	W122	W111−W113	W301−W303
^{17}O	1.07 ± 0.05	0.81 ± 0.02	0.76 ± 0.02
^2H	0.96 ± 0.03	0.81 ± 0.01	0.57 ± 0.01
^1H	0.88 ± 0.05	0.74 ± 0.05	0.52 ± 0.04

[a] In the case of G36S and Y35G, the entries refer to the rms order parameter $\langle A^2\rangle^{1/2}$ averaged over the three buried water molecules.

For W122 in wild-type BPTI, we obtain $\chi(^2H) = 225$ kHz (as in ice Ih). The ^{17}O quadrupole coupling constant is then obtained from an empirical linear relation[51] between $\chi(^{17}O)$ and $\chi(^2H)$, based on data from ice polymorphs and crystal hydrates. Finally, we make the approximation $\langle CA^2\rangle \approx \langle C\rangle\langle A^2\rangle$ in eq 3. In this way we obtain the ^2H and ^{17}O rms order parameters $A \equiv \langle A^2\rangle^{1/2}$ collected in Table 3. Note that the maximum value of A, corresponding to a rigidly (nonrotationally) bound water molecule without librational averaging, is $A_0 = (1 + \eta^2/3)^{1/2}$, which equals 1.00 for ^1H and ^2H but 1.14 for ^{17}O.

The amplitude parameter β obtained by fitting eq 1 to the ^1H dispersion data can be decomposed into three parts as[34]

$$\beta = \beta_{intra} + 0.9\beta_{inter} + \beta_{labile} \qquad (4)$$

corresponding to the intramolecular and intermolecular dipole couplings of the water protons and the direct contribution from rapidly exchanging labile protons. The intramolecular part, β_{intra}, can be expressed as in eq 3 with $C = (10/3)\, M_2^{intra}$. The second moment used for the scaling in Figure 4 was the total (intra + inter), motionally averaged second moment for ice Ih. When corrected for librational averaging, the rigid-lattice limit of the intramolecular moment becomes $M_2^{intra} = 23.3\ G^2$.[48] Since this quantity shows little variation (ca. 3%) among the ice polymorphs, the intramolecular H−H separation cannot depend much on the hydrogen bond geometry.[48,52] Accordingly, we use this M_2^{intra} value for all the buried water molecules.

The intermolecular contribution in eq 4 can be expressed as $\beta_{inter} = (20/9)(N/N_T)\langle M_2^{inter}\rangle$, where the intermolecular second moment (averaged over N buried water molecules) can be calculated from the crystal structure as described elsewhere.[34] Averaging over the four buried water molecules in wild-type BPTI, we thus obtained $\langle M_2^{inter}\rangle = 13.3\ G^2$,[34] to be compared with $M_2^{inter} = 12.8\ G^2$ in ice Ih and $12.1\ G^2$ in ice Ic.[48] To calculate $\langle M_2^{inter}\rangle$ for the three buried water molecules in Y35G, it is necessary to add hydrogens to the protein and water molecules in the X-ray structure.[38] The uncertainty thus introduced is probably comparable to the variation in $\langle M_2^{inter}\rangle$ between G36S and Y35G. We therefore use the value $13.3\ G^2$ also for Y35G, allowing for 10% uncertainty.

Finally, we calculate the direct labile-proton contribution β_{labile} as described previously,[34] using known hydrogen exchange rate constants and interproton distances from the crystal structure. At the present protein concentration ($N_T = 2140$), we thus obtain $\beta_{labile} = 2.2 \times 10^7\ s^{-2}$ for G36S and, after subtraction of the contribution from the hydroxyl proton in Tyr35, $2.0 \times 10^7\ s^{-2}$ for Y35G. We assign a 10% uncertainty to these estimates of β_{labile}. In this way we arrive at the ^1H rms order parameters $A \equiv \langle A^2\rangle^{1/2}$ quoted in Table 3.

The generalized order parameters in Table 3 are model-independent quantities, deduced from the NMRD data without making any assumptions about the nature of the "internal motions" of buried water molecules, except that these motions are fast compared to protein tumbling (6−10 ns, cf. Table 2), as is certainly the case for librational motions. On the other

hand, water motions that are slower than protein tumbling do not affect the spin relaxation rate. The flipping of a buried water molecule 180° around its C_2 axis is usually in this category as are the motions that constitute the actual exchange event. Nevertheless, buried water exchange can affect the measured spin relaxation rate even if it is much slower than protein tumbling. This is the case if the mean residence time (the inverse exchange rate) is not much shorter than the intrinsic spin relaxation time at zero frequency,[20] about 5 μs, 0.3 ms, and 5 ms for ^{17}O, ^{2}H, and ^{1}H, respectively, under the present conditions. The fast-exchange limit assumed in the derivation eq 3 is then no longer applicable. If eq 3 is used under such conditions, it will produce an apparent order parameter that is smaller than the true value. If NMRD profiles are recorded at different temperatures, it can be established whether a buried water molecule is in the fast-exchange limit. For the deeply buried water molecule W122 in wild-type BPTI, it was thus found that the residence time is between the intrinsic relaxation times of ^{17}O and ^{2}H at room temperature.[22] The ^{17}O and ^{2}H order parameters for W122 included in Table 3 were obtained from temperature-dependent difference dispersions and by taking intermediate-exchange effects into account.[22] For ^{1}H, the fast-exchange limit is applicable at 27 °C even for W122.[34] In using eq 3 to derive order parameters, we assume that the six buried water molecules in the G36S and Y35G mutants are in the fast-exchange limit for all three nuclei at 27 °C. Although not demonstrated explicitly, this assumption is supported by the crystal structures, suggesting that W122 exchanges more slowly than the other buried water molecules. Furthermore, a deviation from the fast-exchange limit would mainly suppress the (apparent) order parameter for ^{17}O (since this nucleus has the shortest intrinsic relaxation time). Such a trend is not evident in Table 3.

Libration Amplitudes for Buried Water Molecules. If the orientational disorder of the buried water molecules is anisotropic, we expect the A/A_0 ratios for the three nuclei to differ. The results in Table 3 show that this is the case for both mutants. Moreover, the buried waters in Y35G appear to be significantly more disordered than those in G36S.

To obtain a quantitative measure of the degree and anisotropy of orientational disorder, we introduce a simplified model for the rotational degrees of freedom of buried water molecules. On the relevant subnanosecond time scale, the dominant rotational motions of a buried water molecule are taken to be independent torsional vibrations (librations) around each of three orthogonal axes. The restoring potential is taken to be harmonic so that the libration angles have Gaussian equilibrium distributions. The libration axes are identified with the inertial principal axes, i.e., the three modes correspond to rocking motion (rotation in the molecular plane), wagging motion (tilting of the molecular plane around an axis parallel to the H−H vector), and twisting motion (rotation around the C_2 axis of the water molecule). In addition, we include the possibility of a fast 180° flip around the C_2 axis.

This anisotropic harmonic libration (AHL) model allows us to express the generalized order parameters $A(^{1}\mathrm{H})$, $A(^{2}\mathrm{H})$, and $A(^{17}\mathrm{O})$ as functions of the three rms libration angles $\langle\phi_\alpha^2\rangle^{1/2}$ for the rock ($\alpha = x$), wag ($\alpha = y$), and twist ($\alpha = z$) modes. The explicit results are derived in the Appendix. Figure 5 shows the effect of each libration mode on the generalized order parameters. (A similar plot has been presented previously[33] for ^{2}H and ^{17}O but for a less realistic rectangular ϕ_α distribution.) Some general observations can be made. $A(^{17}\mathrm{O})$ is mainly affected by the twist mode. $A(^{1}\mathrm{H})$ is unaffected by the wag mode and is equally sensitive to rock and twist librations. The C_2 flip only affects $A(^{2}\mathrm{H})$, which is reduced by 40% (in the absence of libration).

TABLE 4: Root-Mean-Square Libration Amplitudes for Buried Water Molecules in Wild-Type BPTI and in the G36S and Y35G Mutants[a]

mode	W122	W111−W113	W301−W303	W301−W303[b]
rock	7 ± 7	9 ± 4	32 ± 2	27 ± 2
wag	5 ± 5	8 ± 8	10 ± 10	5 ± 5
twist	7 ± 7	22 ± 2	21 ± 4	24 ± 2

[a] The tabulated quantity is $\langle\phi_\alpha^2\rangle^{1/2}$ in degrees. [b] Motional averaging by libration modes with the quoted amplitudes and, in addition, by a fast C_2 flip for one of the three water molecules.

In general, of course, all three libration modes are expected to be more or less excited. The relations derived in the Appendix are valid for this general case. Since we have three independent order parameters, the three libration amplitudes can be obtained by numerical inversion of these relations. The results of this operation are presented in Table 4, including propagated errors.[53] The large relative uncertainties for the wag amplitude reflect the insensitivity of $A(^{1}\mathrm{H})$ and $A(^{17}\mathrm{O})$ to this mode (cf. Figure 5). Typically, two of the libration amplitudes are strongly correlated (large covariance).

Several interesting conclusions emerge from the results in Table 4. For the singly buried W122, the libration amplitudes are essentially the same as in ice Ih.[49] This is not unexpected, since W122 makes four hydrogen bonds to backbone atoms in a nearly tetrahedral geometry.[36] For the three buried water molecules in G36S, the twist amplitude is considerably larger than for W122. On the other hand, the G36S order parameters are not consistent with a fast C_2 flip even for one of the three water molecules. Although the twist amplitude is large, the torsional barrier must therefore be sufficiently high to prevent C_2 flips on the time scale of protein tumbling. To make $\tau_{\mathrm{flip}} >$ 10 ns, the flip barrier should exceed ca. 35 kJ mol^{-1}, as in most crystal hydrates and in ice (61 kJ mol^{-1}).[54]

The buried water molecules in Y35G differ from those in G36S mainly in having a large rock amplitude. In contrast to G36S, the Y35G order parameters are consistent with a fast C_2 flip for *one* of the three water molecules. Inclusion of the flip, however, does not alter the libration amplitudes much. Since W303 and W111 are in nearly corresponding locations with very similar hydrogen-bond geometry (cf. Figures 1 and 2 and Table 1), the higher disorder in Y35G can probably be ascribed to W301 and W302 versus W112 and W113 in G36S. Three of these water molecules make four strong hydrogen bonds, but W301 makes only three (cf. Figures 1 and 2b and Table 1). Moreover, the single hydrogen bond accepted by W301 is stronger than the two it donates, a rare occurrence for buried water molecules. These geometrical features suggest that W301 is considerably more disordered than the other three water molecules and, possibly, that it has an unusually low flip barrier, as found for water molecules with single lone-pair coordination in crystal hydrates.[54] The finding that at least one of the buried water molecules in Y35G is considerably more disordered than those in G36S is consistent with the more disordered loops[38] and uniformly faster hydrogen exchange[42] in Y35G.

The results in Table 4 may be somewhat biased by the simplifying assumptions made in the analysis. First, the decomposition into libration modes in the AHL model, while intuitively reasonable, does not take into account the actual force fields experienced by the buried water molecules. Second, in the case of the G36S and Y35G mutants, the libration amplitudes were derived from the squared order parameter A^2 averaged over three buried water molecules, which was regarded as the A^2 value of an "average" buried water molecule. This procedure

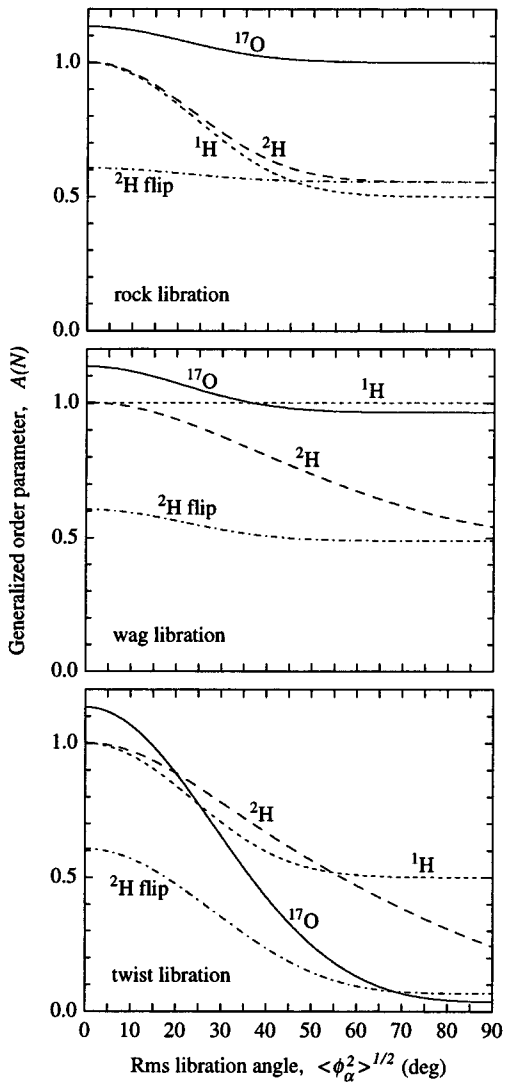

Figure 5. Variation of the generalized order parameters $A(^1H)$, $A(^2H)$, and $A(^{17}O)$ with the rms libration angle for the individual rock (top), wag (middle), and twist (bottom) libration modes in the AHL model. The effect of a fast C_2 flip on $A(^2H)$ is also shown. The geometrical coefficients σ_p were calculated with $\theta_{HOH} = 107°$, $\eta(^2H) = 0.11$, and $\eta(^{17}O) = 0.93$, as in ice Ih.

is clearly not rigorous. Nevertheless, we believe that neither the general conclusions nor the rotational entropy estimates presented below are seriously compromised by these simplifications.

Thermodynamics of Cavity Hydration. According to classical statistical mechanics,[55] the orientational distributions $f(\phi_\alpha)$ that determine the order parameters $A(N)$ are associated with a configurational entropy (per molecule)

$$S_{config} = -k_B \sum_\alpha \int d\phi_\alpha f(\phi_\alpha) \ln f(\phi_\alpha) \qquad (5)$$

Owing to the small moments of inertia of the water molecule, quantum corrections are important and the rotational entropy S_R (per molecule) for the AHL model is given more accurately by[31,56]

$$S_R = -k_B \sum_\alpha \left\{ \frac{C_\alpha}{\exp(C_\alpha) - 1} - \ln[1 - \exp(-C_\alpha)] \right\} \qquad (6)$$

with the dimensionless quantity $C_\alpha = \hbar\omega_\alpha/(k_B T)$ related to the mode amplitudes $\langle\phi_\alpha{}^2\rangle^{1/2}$ and the moments of inertia I_α through

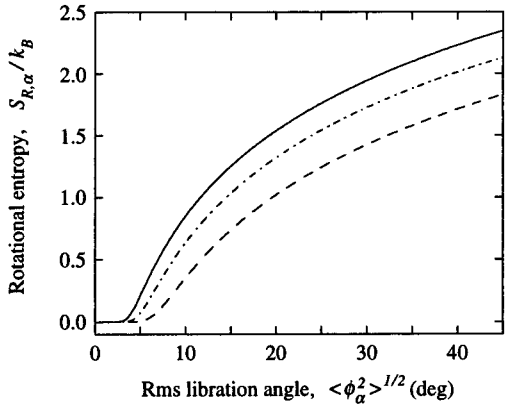

Figure 6. Rotational entropy for the rock (solid curve), wag (dash), and twist (dash−dot) libration modes in the AHL model calculated from eqs 6 and 7 with moments of inertia for H_2O.

$$\langle\phi_\alpha{}^2\rangle = \frac{\hbar^2}{2k_B T I_\alpha} \frac{\coth(C_\alpha/2)}{C_\alpha} \qquad (7)$$

Figure 6 shows how the rotational entropy contributions $S_{R,\alpha}$ increase with the libration amplitudes $\langle\phi_\alpha{}^2\rangle^{1/2}$ for the three modes in the AHL model. With the aid of these relations, we can convert[57] the experimentally derived libration amplitudes in Table 4 to rotational entropies. We thus obtain $S_R = 0.8k_B$ (W122), $2.3k_B$ (average over W111−W113), and $3.7k_B$ (average over W301−W303). (With the libration amplitudes in the last column of Table 4, the last figure becomes $3.3k_B$.[58]) Compared to the ice-like W122, the buried water molecules in G36S and Y35G thus enjoy considerable entropic stabilization.

The free energy ΔG associated with the transfer of a water molecule from bulk water to a protein cavity determines the fractional occupancy f of the cavity according to

$$\Delta G = \Delta H - T\Delta S = -k_B T \ln[f/(1 - f)] \qquad (8)$$

The entropy of transfer is $\Delta S = S_{cav} - S_{bulk}$, where $S_{bulk} = 8.4k_B$ is the entropy of bulk water at 300 K.[59] (Any changes in the vibrational entropy of the protein upon cavity hydration are neglected here.) Since W122 has ice-like hydrogen-bond geometry[36] and ice-like libration amplitudes (vide supra), we set $S_{cav}(W122) = 5.0k_B$, the entropy of a water molecule in ice Ih.[59,60] The entropy of water in most inorganic crystal hydrates is within 10% of this value.[61] Furthermore, since all buried water molecules considered here are highly positionally ordered relative to the protein,[36,38,62] we assume that they have the same translational entropy. After these simplifications, we have (for a buried water molecule denoted Wx): $\Delta S(Wx) = S_R(Wx) - S_R(W122) + S_{ice} - S_{bulk} = S_R(Wx) - 4.2k_B$. With the S_R values quoted above, we thus obtain for the entropic cost of transferring a water molecule from bulk water to the protein cavity $\Delta S = -3.4k_B$ for W122, $-1.9k_B$ for G36S, and $-0.5k_B$ for Y35G.

Our analysis thus indicates that the three buried water molecules in Y35G, despite extensive hydrogen bonding, have nearly the same entropy (on average) as in bulk water. This suggests that for many other, less extensively hydrogen-bonded internal water molecules, entropy is actually a driving force for cavity hydration. More than 60% of the internal water molecules *detected* in protein crystal structures make less than four hydrogen bonds, and 20% make less than three.[3] Furthermore, recent high-resolution ^1H NMR studies of intermolecular NOEs indicate that some protein cavities that appear empty in X-ray diffraction are at least partially occupied.[21,27] (If the X-ray invisibility is due to positional disorder, the translational entropy would further add to the driving force for cavity hydration.)

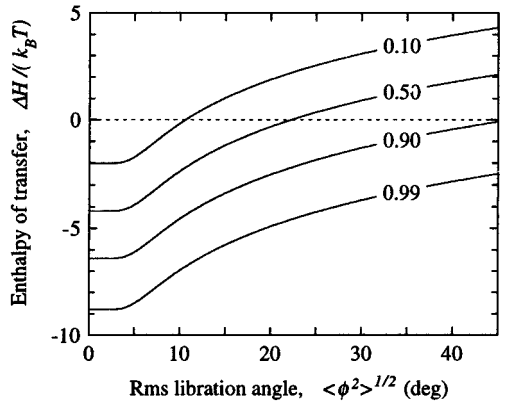

Figure 7. Enthalpy−entropy compensation in the free energy of cavity hydration. For a cavity where a water molecule is orientationally disordered to the extent given by the rms libration angle (and has the same translational entropy as in ice), the curves represent the enthalpy cost for attaining the indicated occupancies.

To illustrate the quantitative aspects of this enthalpy−entropy compensation effect on cavity hydration, we have calculated $\Delta S = S_R - 4.2k_B$ as a function of the libration amplitude, with S_R obtained from eqs 6 and 7. For this calculation, we use the same libration amplitude for the three modes.[63] We then use eq 8 to calculate the enthalpy of transfer ΔH required for a given cavity occupancy *f*. As seen from Figure 7, a significant occupancy can be achieved at a small enthalpy cost even for moderately orientationally disordered water molecules. For 50% occupancy, for example, $\Delta H = 0$ for a libration amplitude of about 20°. In the absence of librational motion in the cavity, the enthalpy cost for 50% occupancy is $4.2k_BT$, or 2.5 kcal mol^{-1}. For strongly hydrogen-bonded water molecules like W122, of course, $-\Delta H$ is expected to be considerably larger, yielding nearly 100% occupancy.

The picture of cavity hydration that emerges from the present analysis is consistent with recent reports of water in protein cavities with little or no hydrogen-bonding capacity.[21,26,27] It may also explain the intriguing theoretical result of an atomic force-field calculation, that a water molecule may be transferred from bulk water into a weakly hydrogen-bonding protein cavity without any significant free energy cost.[23] Extensive enthalpy−entropy compensation in cavity hydration is also suggested by a statistical analysis[3] of crystallographic data, showing that a hydrogen bond reduces the *free* energy of a buried water molecule by merely 0.6 kcal mol^{-1} (on average).

According to conventional wisdom, protein-associated water is more ordered than bulk water. The entropic gain on displacement of such ordered water molecules is widely held to facilitate protein−ligand and protein−receptor association.[13,64−69] When association involves extensive hydrophobic areas, this is undoubtedly a valid picture (at least near room temperature). In many other cases, however, water displacement may well be accompanied by an entropy loss. We expect this to be the case for weakly hydrogen-bonded water molecules in narrow pockets or crevices on the protein surface. It has recently been pointed out that protein-associated water should not be much more ordered than bulk water, since the entropy difference between bulk water and ice (or most crystal hydrates) is merely $3.4k_B$.[61] The translational disorder at the protein−water interface implied by large crystallographic *B* factors also suggests that part of the surface hydration may not be significantly more (translationally) ordered than bulk water.[68] Our analysis focuses on the *rotational* degrees of freedom, which appear to dominate the relevant entropy changes, and goes further by proposing that some protein-associated water molecules may be *less* ordered than bulk water. Such water molecules can be expected in weakly hydrogen-bonded internal cavities and narrow surface pockets and may be of particular importance for protein stability and association processes.

Conclusions

The present multinuclear water NMRD data for the BPTI mutant Y35G demonstrate that the three internal water molecules exchange on a time scale of 15 ns to 1 μs. A comparison with analogous NMRD data[19,34] for the mutant G36S shows that the buried water molecules in Y35G are more disordered than those in G36S. With the aid of an anisotropic harmonic libration model, the three independent order parameters provided by the NMRD data were transformed into rms angular amplitudes for the rock, wag, and twist libration modes. The same model was then used to estimate the associated rotational entropy contributions for the buried water molecules. On the assumption that the translational entropy of the investigated buried water molecules is essentially the same as in ice, it was concluded that the buried water molecules in Y35G, despite extensive hydrogen-bonding to the protein, do not have significantly lower entropy than bulk water. This finding appears to have interesting implications for the understanding of the thermodynamics of cavity hydration, protein−ligand association, and protein stability.

Acknowledgment. This work was supported by the Swedish Natural Science Research Council and the Swedish Council for Planning and Coordination of Research.

Appendix: Generalized Order Parameters for the Anisotropic Harmonic Libration Model

The generalized order parameters *A*(N), with N = ^{1}H, ^{2}H, or ^{17}O, describe the effect on the megahertz relaxation dispersion of any reorientational motion of a buried water molecule that is fast compared to the isotropic tumbling of the protein. Since the nuclear interaction tensors have different orientations with respect to the water molecule, the three generalized order parameters provide independent information about the internal motion. This information is contained in the second-rank orientational order parameters

$$S_{np} = \int \mathrm{d}\Omega\, f(\Omega) D^2_{np}(\Omega) \qquad \text{(A1)}$$

which determine the *A*(N) according to[33]

$$A^2(\mathrm{N}) = \sum_n |\sum_p \sigma_p(\mathrm{N}) S_{np}|^2 \qquad \text{(A2)}$$

The nucleus-specific geometrical coefficients σ_p(N) have been given elsewhere for ^{2}H and ^{17}O.[33] For ^{1}H they are $\sigma_0 = -1/2$, $\sigma_{\pm 1} = 0$, and $\sigma_{\pm 2} = -\sqrt{6}/4$.

In the anisotropic harmonic libration (AHL) model, the internal motion is modeled in terms of three independent symmetric libration modes: (i) the rocking of the water molecule around an axis perpendicular to the molecular plane, (ii) the wagging of the water molecule around an axis parallel to the H−H vector, and (iii) the twisting of the water molecule around its C_2 axis. For all modes, the rotation axis passes through the oxygen atom. In addition, we include the possibility of a 180° flip around the C_2 axis.

In eq A1, $D^2_{np}(\Omega)$ is a Wigner function[70] and Ω denotes the set of three Euler angles that specifies the transformation between a frame fixed in the water molecule (with the *z* axis along the C_2 axis and the *x* axis perpendicular to the molecular

plane) and a frame that coincides with the molecular frame in the equilibrium configuration (zero libration angles). In the AHL model, the angular variables are the libration angles ϕ_x, ϕ_y, and ϕ_z for the rock, wag, and twist modes, respectively. The order parameters S_{np} can be expressed in terms of these variables as

$$S_{np} = \delta_{n+p,\text{even}} \langle \cos(n\phi_z) \rangle \sum_q \delta_{q+p,\text{even}} (-1)^{(p-q)/2} \times \langle d^2_{nq}(\phi_y) \rangle \langle d^2_{qp}(\phi_x) \rangle \quad \text{(A3)}$$

where the angular brackets denote averages over the appropriate equilibrium distribution $f(\phi_\alpha)$, $\alpha = x$, y, or z. Owing to the noncommutability of finite rotations, the order parameters in the AHL model depend on the order in which the rotations are applied. (The result in eq A3 corresponds to the order ϕ_x first and ϕ_z last.) For the libration amplitudes of interest here, however, this dependence is very weak and can be neglected.

On account of the symmetry of the libration modes (with respect to $\phi_\alpha = 0$), there are only five (rather than 25) independent order parameters, namely,

$$S_{00} = 1 - \frac{3}{2}[\langle \sin^2 \phi_x \rangle + \langle \sin^2 \phi_y \rangle - \langle \sin^2 \phi_x \rangle \langle \sin^2 \phi_y \rangle] \quad \text{(A4a)}$$

$$S_{02} = -\frac{\sqrt{6}}{4}[-\langle \sin^2 \phi_x \rangle + \langle \sin^2 \phi_y \rangle + \langle \sin^2 \phi_x \rangle \langle \sin^2 \phi_y \rangle] \quad \text{(A4b)}$$

$$S_{20} = \frac{\sqrt{6}}{4}[1 - 2\langle \sin^2 \phi_z \rangle] \times [-\langle \sin^2 \phi_x \rangle + \langle \sin^2 \phi_y \rangle - \langle \sin^2 \phi_x \rangle \langle \sin^2 \phi_y \rangle] \quad \text{(A4c)}$$

$$S_{22} + S_{2-2} = \frac{1}{2}[1 - 2\langle \sin^2 \phi_z \rangle] \times [2 - \langle \sin^2 \phi_x \rangle - \langle \sin^2 \phi_y \rangle - \langle \sin^2 \phi_x \rangle \langle \sin^2 \phi_y \rangle] \quad \text{(A4d)}$$

$$S_{11} + S_{1-1} = \langle \cos \phi_z \rangle \langle \cos \phi_y \rangle [1 - 2\langle \sin^2 \phi_x \rangle] \quad \text{(A4e)}$$

In the presence of a C_2 flip, the order parameters S_{np} must also reflect the C_{2v} symmetry of the water molecule, which requires p to be even. The only effect of the flip is thus to make $S_{11} + S_{1-1} = 0$.

In the AHL model, the five order parameters in eq A4 are not independent. They are all determined by three parameters, which we take as the rms amplitudes $\langle \phi_\alpha^2 \rangle^{1/2}$ of the libration modes. The orientational distribution function for each mode is of the form

$$f(\phi_\alpha) = \frac{1}{(2\pi \langle \phi_\alpha^2 \rangle)^{1/2}} \exp\left(-\frac{\phi_\alpha^2}{2\langle \phi_\alpha^2 \rangle}\right) \quad \text{(A5)}$$

This distribution is normalized on the unrestricted interval $-\infty < \phi_\alpha < \infty$, rather than on $-\pi \le \phi_\alpha \le \pi$. The error introduced by this approximation is negligible for the libration amplitudes of interest here (say, $\langle \phi_\alpha^2 \rangle^{1/2} < 45°$). For the Gaussian distribution A5, the five order parameters in eq A4 can be expressed in terms of the orientational averages

$$\langle \cos(n\phi_\alpha) \rangle = \exp\left(-\frac{n^2}{2}\langle \phi_\alpha^2 \rangle\right) \quad \text{(A6)}$$

with $n = 1$ or 2.

In the rigid-lattice limit, i.e., in the absence of librational motion, we have $S_{np} = \delta_{np}$ and the preceding results for the AHL model reduce correctly to

$$A^2(\text{N}) = 1 + \eta^2(\text{N})/3 \quad \text{(A7)}$$

with η the asymmetry parameter of the nuclear interaction tensor.

In the free-rotation limit, with a uniform ϕ_α distribution, the AHL model yields $A^2(\text{N}) = [\sigma_0(\text{N}) - \sqrt{6}\sigma_2(\text{N})]^2/4$ for the rock mode, $A^2(\text{N}) = [\sigma_0(\text{N}) + \sqrt{6}\sigma_2(\text{N})]^2/4$ for the wag mode, and $A^2(\text{N}) = [\sigma_0(\text{N})]^2$ for the twist mode.[33] If all three libration angles are uniformly distributed, the AHL model yields $A^2(\text{N}) = [\sigma_0(\text{N}) - \sqrt{6}\sigma_2(\text{N})]^2/64$, i.e., $A(^1\text{H}) = {}^1/_8$, $A(^2\text{H}) = (1 + \eta)/8$, and $A(^{17}\text{O}) = {}^1/_4$. This differs from the isotropic limit, where $A(\text{N}) = 0$. The difference is unimportant, however, for the libration amplitudes of interest here.

References and Notes

(1) Connolly, M. L. *Int. J. Pept. Protein Res.* **1985**, *28*, 360−363.
(2) Rashin, A. A.; Iofin, M.; Honig, B. *Biochemistry* **1986**, *25*, 3619−3625.
(3) Williams, M. A.; Goodfellow, J. M.; Thornton, J. M. *Protein Sci.* **1994**, *3*, 1224−1235.
(4) Hubbard, S. J.; Gross, K.-H.; Argos, P. *Protein Eng.* **1994**, *7*, 613−626. Hubbard, S. J.; Argos, P. *Protein Eng.* **1995**, *8*, 1011−1015.
(5) Baker, E. N. In *Protein-Solvent Interactions*; Gregory, R. B., Ed.; M. Dekker: New York, 1995; Chapter 2.
(6) Schoenborn, B. P.; Garcia, A.; Knott, R. *Prog. Biophys. Mol. Biol.* **1995**, *64*, 105−119.
(7) McDowell, R. S.; Kossiakoff, A. A. *J. Mol. Biol.* **1995**, *250*, 553−570.
(8) Elber, R.; Karplus, M. *J. Am. Chem. Soc.* **1990**, *112*, 9161−9175.
(9) Carlson, M. L.; Regan, R. M.; Gibson, Q. H. *Biochemistry* **1996**, *35*, 1125−1136.
(10) Gerstein, M.; Lesk, A. M.; Chothia, C. *Biochemistry* **1994**, *33*, 6739−6749.
(11) Hubbard, S. J.; Argos, P. *J. Mol. Biol.* **1996**, *261*, 289−300.
(12) Meyer, E. *Protein Sci.* **1992**, *1*, 1543−1562.
(13) Ladbury, J. E. *Chem. Biol.* **1996**, *3*, 973−980.
(14) Raymer, M. L.; Sanschagrin, P. C.; Punch, W. F.; Venkataraman, S.; Goodman, E. D.; Kuhn, L. A. *J. Mol. Biol.* **1997**, *265*, 445−464.
(15) Otting, G.; Wüthrich, K. *J. Am. Chem. Soc.* **1989**, *111*, 1871−1875.
(16) Otting, G.; Liepinsh, E.; Wüthrich, K. *Science* **1991**, *254*, 974−980.
(17) Otting, G.; Liepinsh, E. *Acc. Chem. Res.* **1995**, *28*, 171−177.
(18) Denisov, V. P.; Halle, B. *J. Mol. Biol.* **1995**, *245*, 682−697.
(19) Denisov, V. P.; Halle, B.; Peters, J.; Hörlein, H. D. *Biochemistry* **1995**, *34*, 9046−9051.
(20) Denisov, V. P.; Halle, B. *Faraday Discussions* **1996**, *103*, 227−244.
(21) Otting, G.; Liepinsh, E.; Halle, B.; Frey, U. *Nature Struct. Biol.* **1997**, *4*, 396−404.
(22) Denisov, V. P.; Peters, J.; Hörlein, H. D.; Halle, B. *Nature Struct. Biol.* **1996**, *3*, 505−509.
(23) Wade, R. C.; Mazor, M. H.; McCammon, J. A.; Quiocho, F. A. *Biopolymers* **1991**, *31*, 919−931.
(24) Zhang, L.; Hermans, J. *Proteins: Struct. Funct. Gen.* **1996**, *24*, 433−438.
(25) Wolfenden, R.; Radzicka, A. *Science* **1994**, *265*, 936−937.
(26) Buckle, A. M.; Cramer, P.; Fersht, A. R. *Biochemistry* **1996**, *35*, 4298−4305.
(27) Ernst, J. A.; Clubb, R. T.; Zhou, H.-X.; Gronenborn, A. M.; Clore, G. M. *Science* **1995**, *267*, 1813−1817.
(28) Berne, B. J.; Pechukas, P.; Harp, G. D. *J. Chem. Phys.* **1968**, *49*, 3125−3129.
(29) Zannoni, C. In *The Molecular Dynamics of Liquid Crystals*; Luckhurst, G. R., Veracini, C. A., Eds.; Kluwer: Dordrecht, 1994; Chapter 2.
(30) Akke, M.; Brüschweiler, R.; Palmer, A. G. *J. Am. Chem. Soc.* **1993**, *115*, 9832−9833.
(31) Yang, D.; Kay, L. E. *J. Mol. Biol.* **1996**, *263*, 369−382.
(32) Li, Z.; Raychaudhuri, S.; Wand, A. J. *Protein Sci.* **1996**, *5*, 2647−2650.
(33) Denisov, V. P.; Halle, B. *J. Am. Chem. Soc.* **1995**, *117*, 8456−8465.
(34) Venu, K.; Denisov, V. P.; Halle, B. *J. Am. Chem. Soc.* **1997**, *119*, 3122−3134.
(35) Denisov, V. P.; Halle, B. *J. Mol. Biol.* **1995**, *245*, 698−709.

(36) Wlodawer, A.; Walter, J.; Huber, R.; Sjölin, L. *J. Mol. Biol*. **1984**, *180*, 301−329.
(37) Berndt, K. D.; Beunink, J.; Schröder, W.; Wüthrich, K. *Biochemistry* **1993**, *32*, 4564−4570.
(38) Housset, D.; Kim, K.-S.; Fuchs, J.; Woodward, C.; Wlodawer, A. *J. Mol. Biol*. **1991**, *220*, 757−770.
(39) Lumry, R.; Rajender, S. *Biopolymers* **1970**, *9*, 1125−1227.
(40) Dunitz, J. D. *Chem. Biol*. **1995**, *2*, 709−712.
(41) Berndt, K. D.; Güntert, P.; Orbons, L. P. M.; Wüthrich, K. *J. Mol. Biol.* **1992**, *227*, 757−775.
(42) Kim, K.-S.; Fuchs, J. A.; Woodward, C. K. *Biochemistry* **1993**, *32*, 9600−9608.
(43) Abragam, A. *The Principles of Nuclear Magnetism*: Clarendon Press: Oxford, 1961.
(44) Halle, B.; Wennerström, H. *J. Magn. Reson*. **1981**, *44*, 89−100.
(45) Halle, B.; Wennerström, H. *J. Chem. Phys*. **1981**, *75*, 1928−1943.
(46) Spiess, H. W.; Garrett, B. B.; Sheline, R. K.; Rabideau, S. W. *J. Chem. Phys*. **1969**, *51*, 1201−1205. Edmonds, D. T.; Zussman, A. *Phys. Lett*. **1972**, *41A*, 167−169.
(47) Edmonds, D. T.; Mackay, A. L. *J. Magn. Reson*. **1975**, *20*, 515−519.
(48) Whalley, E. *Mol. Phys*. **1974**, *28*, 1105−1108.
(49) Sceats, M. G.; Rice, S. A. *J. Chem. Phys*. **1980**, *72*, 3236−3247.
(50) Berglund, B.; Lindgren, J.; Tegenfeldt, J. *J. Mol. Struct*. **1978**, *43*, 179−191.
(51) Poplett, I. J. F. *J. Magn. Reson*. **1982**, *50*, 397−408.
(52) Kuhs, W. F.; Lehmann, M. S. *Water Sci. Rev.* **1986**, *2*, 1−65.
(53) The libration amplitude bounds in Table 4 are mainly determined by $A(^2\mathrm{H})$ and $A(^{17}\mathrm{O})$ and depend only weakly on the less precisely defined $A(^1\mathrm{H})$. If the estimated uncertainties in $\langle M_2^{\mathrm{inter}} \rangle$ and β_{labile} are taken to be 20% rather than 10%, the propagated error in $A(^1\mathrm{H})$ is doubled but the effect on the libration amplitudes is barely significant. For Y35G (without C_2 flip), for example, we obtain $32 \pm 2°$, $13 \pm 13°$, and $20 \pm 5°$ for 20% uncertainty in $\langle M_2^{\mathrm{inter}} \rangle$ and β_{labile}, compared with the values in the fourth column of Table 4.
(54) Larsson, K.; Tegenfeldt, J.; Hermansson, K. *J. Chem. Soc., Faraday Trans*. **1991**, *87*, 1193−1200.
(55) Hill, T. L. *An Introduction to Statistical Thermodynamics*; Dover: New York, 1986.
(56) Landau, L. D.; Lifshitz, E. M. *Statistical Physics*, 3rd ed.; Pergamon: Oxford, 1980; Part 1.
(57) All thermodynamic quantities refer to H_2O. With its twice as large moments of inertia, D_2O should have 10−15% larger libration amplitudes. Since this difference is comparable to or smaller than the propagated uncertainties in Table 4, we ignore the isotope effect.
(58) Since the C_2 flip interconverts two indistinguishable states, there is no associated configurational entropy.
(59) Eisenberg, D.; Kauzmann, W. *The Structure and Properties of Water*; Clarendon: Oxford, 1969.
(60) The entropy of ice Ih at 273 K is $5.0k_B$ from which a contribution of $0.4k_B$, due to residual proton disorder, should be subtracted and another contribution of $0.4k_B$, from the extrapolation to 300 K (using the heat capacity of ice Ih), should be added.[59]
(61) Dunitz, J. D. *Science* **1994**, *264*, 670.
(62) The Debye−Waller factors for the water oxygens are 11.1 Å^2 (W122), 13.4 Å^2 (average for W111−W113), and 9.1 Å^2 (average for W301−W303).[36,38] To compensate for differences in lattice disorder between the BPTI and Y35G crystals, the difference, $7 - 2 = 5$ Å^2, between the smallest *B* factors in the two proteins should be added to the latter value.[71]
(63) For relatively large libration amplitudes, this is actually no restriction, since the classical limit of eq 6 depends only on the geometric average of the three libration amplitudes.
(64) Finkelstein, A. V.; Janin, J. *Protein Eng*. **1989**, *3*, 1−3.
(65) Searle, M. S.; Williams, D. H. *J. Am. Chem. Soc*. **1992**, *114*, 10690−10697.
(66) Gilli, P.; Ferretti, V.; Gilli, G.; Borea, P. A. *J. Phys. Chem*. **1994**, *98*, 1515−1518.
(67) Chervenak, M. C.; Toone, E. J. *J. Am. Chem. Soc*. **1994**, *116*, 10533−10539.
(68) Ringe, D. *Curr. Opin. Struct. Biol*. **1995**, *5*, 825−829.
(69) Tame, J. R. H.; Sleigh, S. H.; Wilkinson, A. J.; Ladbury, J. E. *Nature Struct. Biol*. **1996**, *3*, 998−1001.
(70) Brink, D. M.; Satchler, G. R. *Angular Momentum*, 2nd ed.; Clarendon: Oxford, 1968.
(71) Ringe, D.; Petsko, G. A. *Prog. Biophys. Mol. Biol*. **1985**, *45*, 197−235.
(72) Beeser, S. A.; Goldenberg, D. P.; Oas, T. G. *J. Mol. Biol*. **1997**, *269*, 154−164.